

Search for a scalar bottom quark with mass 3.5–4.5 GeV/ c^2

CLEO Collaboration

(February 7, 2008)

Abstract

We report on a search for a supersymmetric \tilde{B} meson with mass between 3.5 and 4.5 GeV/ c^2 using 4.52 fb $^{-1}$ of integrated luminosity produced at $\sqrt{s} = 10.52$ GeV, just below the $e^+e^- \rightarrow B\tilde{B}$ threshold, and collected with the CLEO detector. We find no evidence for a light scalar bottom quark.

V. Savinov,¹ T. E. Coan,² V. Fadeyev,² Y. S. Gao,² Y. Maravin,² I. Narsky,²
R. Stroynowski,² J. Ye,² T. Wlodek,² M. Artuso,³ R. Ayad,³ C. Boulahouache,³ K. Bukin,³
E. Dambasuren,³ S. Karamov,³ G. Majumder,³ G. C. Moneti,³ R. Mountain,³ S. Schuh,³
T. Skwarnicki,³ S. Stone,³ J.C. Wang,³ A. Wolf,³ J. Wu,³ S. Kopp,⁴ M. Kostin,⁴
A. H. Mahmood,⁵ S. E. Csorna,⁶ I. Danko,⁶ K. W. McLean,⁶ Z. Xu,⁶ R. Godang,⁷
G. Bonvicini,⁸ D. Cinabro,⁸ M. Dubrovin,⁸ S. McGee,⁸ G. J. Zhou,⁸ E. Lipeles,⁹
S. P. Pappas,⁹ M. Schmidtler,⁹ A. Shapiro,⁹ W. M. Sun,⁹ A. J. Weinstein,⁹
F. Würthwein,^{9,*} D. E. Jaffe,¹⁰ G. Masek,¹⁰ H. P. Paar,¹⁰ E. M. Potter,¹⁰ S. Prell,¹⁰
D. M. Asner,¹¹ A. Eppich,¹¹ T. S. Hill,¹¹ R. J. Morrison,¹¹ R. A. Briere,¹² G. P. Chen,¹²
A. Gritsan,¹³ J. P. Alexander,¹⁴ R. Baker,¹⁴ C. Bebek,¹⁴ B. E. Berger,¹⁴ K. Berkelman,¹⁴
F. Blanc,¹⁴ V. Boisvert,¹⁴ D. G. Cassel,¹⁴ P. S. Drell,¹⁴ J. E. Duboscq,¹⁴ K. M. Ecklund,¹⁴
R. Ehrlich,¹⁴ A. D. Foland,¹⁴ P. Gaidarev,¹⁴ R. S. Galik,¹⁴ L. Gibbons,¹⁴ B. Gittelman,¹⁴
S. W. Gray,¹⁴ D. L. Hartill,¹⁴ B. K. Heltsley,¹⁴ P. I. Hopman,¹⁴ L. Hsu,¹⁴ C. D. Jones,¹⁴
J. Kandaswamy,¹⁴ D. L. Kreinick,¹⁴ M. Lohner,¹⁴ A. Magerkurth,¹⁴ T. O. Meyer,¹⁴
N. B. Mistry,¹⁴ E. Nordberg,¹⁴ M. Palmer,¹⁴ J. R. Patterson,¹⁴ D. Peterson,¹⁴ D. Riley,¹⁴
A. Romano,¹⁴ J. G. Thayer,¹⁴ D. Urner,¹⁴ B. Valant-Spaight,¹⁴ G. Viehhauser,¹⁴
A. Warburton,¹⁴ P. Avery,¹⁵ C. Prescott,¹⁵ A. I. Rubiera,¹⁵ H. Stoeck,¹⁵ J. Yelton,¹⁵
G. Brandenburg,¹⁶ A. Ershov,¹⁶ D. Y.-J. Kim,¹⁶ R. Wilson,¹⁶ T. Bergfeld,¹⁷
B. I. Eisenstein,¹⁷ J. Ernst,¹⁷ G. E. Gladding,¹⁷ G. D. Gollin,¹⁷ R. M. Hans,¹⁷ E. Johnson,¹⁷
I. Karliner,¹⁷ M. A. Marsh,¹⁷ C. Plager,¹⁷ C. Sedlack,¹⁷ M. Selen,¹⁷ J. J. Thaler,¹⁷
J. Williams,¹⁷ K. W. Edwards,¹⁸ R. Janicek,¹⁹ P. M. Patel,¹⁹ A. J. Sadoff,²⁰ R. Ammar,²¹
A. Bean,²¹ D. Besson,²¹ X. Zhao,²¹ S. Anderson,²² V. V. Frolov,²² Y. Kubota,²² S. J. Lee,²²
R. Mahapatra,²² J. J. O'Neill,²² R. Poling,²² T. Riehle,²² A. Smith,²² C. J. Stepaniak,²²
J. Urheim,²² S. Ahmed,²³ M. S. Alam,²³ S. B. Athar,²³ L. Jian,²³ L. Ling,²³ M. Saleem,²³
S. Timm,²³ F. Wappler,²³ A. Anastassov,²⁴ E. Eckhart,²⁴ K. K. Gan,²⁴ C. Gwon,²⁴
T. Hart,²⁴ K. Honscheid,²⁴ D. Hufnagel,²⁴ R. Kass,²⁴ T. K. Pedlar,²⁴ H. Schwarthoff,²⁴
J. B. Thayer,²⁴ E. von Toerne,²⁴ M. M. Zoeller,²⁴ S. J. Richichi,²⁵ H. Severini,²⁵ P. Skubic,²⁵
A. Undrus,²⁵ S. Chen,²⁶ J. Fast,²⁶ J. W. Hinson,²⁶ J. Lee,²⁶ D. H. Miller,²⁶ E. I. Shibata,²⁶
I. P. J. Shipsey,²⁶ V. Pavlunin,²⁶ D. Cronin-Hennessy,²⁷ A.L. Lyon,²⁷ and E. H. Thorndike²⁷

¹Stanford Linear Accelerator Center, Stanford University, Stanford, California 94309

²Southern Methodist University, Dallas, Texas 75275

³Syracuse University, Syracuse, New York 13244

⁴University of Texas, Austin, TX 78712

⁵University of Texas - Pan American, Edinburg, TX 78539

⁶Vanderbilt University, Nashville, Tennessee 37235

⁷Virginia Polytechnic Institute and State University, Blacksburg, Virginia 24061

⁸Wayne State University, Detroit, Michigan 48202

⁹California Institute of Technology, Pasadena, California 91125

¹⁰University of California, San Diego, La Jolla, California 92093

¹¹University of California, Santa Barbara, California 93106

¹²Carnegie Mellon University, Pittsburgh, Pennsylvania 15213

*Permanent address: Massachusetts Institute of Technology, Cambridge, MA 02139.

- ¹³University of Colorado, Boulder, Colorado 80309-0390
¹⁴Cornell University, Ithaca, New York 14853
¹⁵University of Florida, Gainesville, Florida 32611
¹⁶Harvard University, Cambridge, Massachusetts 02138
¹⁷University of Illinois, Urbana-Champaign, Illinois 61801
¹⁸Carleton University, Ottawa, Ontario, Canada K1S 5B6
and the Institute of Particle Physics, Canada
¹⁹McGill University, Montréal, Québec, Canada H3A 2T8
and the Institute of Particle Physics, Canada
²⁰Ithaca College, Ithaca, New York 14850
²¹University of Kansas, Lawrence, Kansas 66045
²²University of Minnesota, Minneapolis, Minnesota 55455
²³State University of New York at Albany, Albany, New York 12222
²⁴Ohio State University, Columbus, Ohio 43210
²⁵University of Oklahoma, Norman, Oklahoma 73019
²⁶Purdue University, West Lafayette, Indiana 47907
²⁷University of Rochester, Rochester, New York 14627

There has recently been renewed interest in the possibility of a light scalar bottom quark [1], which ALEPH has searched for [2]. It has been noted that such a squark can exist in certain regions of parameter space [3]. In addition, the production cross section of scalar quarks in e^+e^- annihilations, well above threshold, is $\frac{1}{4}$ that of spin- $\frac{1}{2}$ quarks of the same charge; thus $\tilde{b}\tilde{b}^*$ production would contribute $\frac{1}{12}$ unit to R , the ratio of hadronic cross section to $\mu^+\mu^-$ cross section, and such an increase cannot be ruled out by existing measurements [4]. Indirect evidence from the measured B semileptonic branching fraction disfavors the existence of a light \tilde{b} [5].

If \tilde{b} is the lightest supersymmetric particle (LSP), and if R -parity is conserved, then \tilde{b} would be stable. If, instead, a scalar neutrino $\tilde{\nu}$ is the LSP, then \tilde{b} will decay $\tilde{b} \rightarrow c\ell^-\tilde{\nu}$ and/or $\tilde{b} \rightarrow u\ell^-\tilde{\nu}$. If R -parity is violated, \tilde{b} will decay $\tilde{b} \rightarrow c\ell^-$ and/or $\tilde{b} \rightarrow u\ell^-$. We have searched for a light \tilde{b} that decays $\tilde{b} \rightarrow c\ell^-\tilde{\nu}$ and/or $\tilde{b} \rightarrow c\ell^-$. Such a particle would dress itself as a supersymmetric \tilde{B} meson. The dressed decays would be $\tilde{B} \rightarrow DX\ell^-\tilde{\nu}$ and $\tilde{B} \rightarrow DX\ell^-$, where X represents possible additional conventional hadrons.

The decays we search for, characterized by leptons and charmed mesons, have much in common with conventional B decays. We perform a direct search, avoiding the B background by using a data sample collected below the $B\tilde{B}$ threshold, at $\sqrt{s} = 10.52$ GeV. Our search covers the \tilde{B} mass range 3.5–4.5 GeV/ c^2 . Because our search is near $\tilde{B}\tilde{B}^*$ threshold, the production cross section cannot be predicted with great precision. We include the β^3 threshold factor and ignore strong interaction effects to obtain $\sigma(e^+e^- \rightarrow \tilde{b}\tilde{b}^*) = N_c\pi\alpha^2Q_f^2\beta^3/3s$ (derived from Eq. 35.12 of Ref. [6]), where Q_f , the charge of the \tilde{b} , is $-\frac{1}{3}$.

Below $B\tilde{B}$ threshold, the major source of leptons and charmed mesons is $e^+e^- \rightarrow c\bar{c}$, which predominantly produces two charged leptons when both charmed mesons decay semileptonically. To suppress this $c\bar{c}$ background, we search for events with two oppositely charged leptons as well as a fully reconstructed hadronic D or D^* meson decay, where $D^{(*)}$ denotes either a $D^{(*)0}$ or $D^{(*)+}$ meson. Other sources of leptons include kaons that decay in flight, photon conversions, and π^0 Dalitz decays. A search for wrong-sign $D^{(*)}$ -lepton combinations was also conducted, but the resultant upper limits were significantly weaker than for the $D^{(*)}$ -dilepton signature, and they are not discussed further in this paper.

The data sample used in this analysis was produced in symmetric e^+e^- collisions at the Cornell Electron Storage Ring (CESR) and collected with the CLEO detector in two configurations, known as CLEO II [7] and CLEO II.V [8]. It comprises 4.52 fb $^{-1}$ of integrated luminosity produced at an e^+e^- center-of-mass energy of $\sqrt{s} = 10.52$ GeV, 35 MeV below the $B\tilde{B}$ threshold. Analysis of an additional 2.24 fb $^{-1}$ collected on the $\Upsilon(4S)$ resonance provides a sample of B mesons, which can mimic the behavior of \tilde{B} mesons, thus allowing us to verify our experimental technique. The response of the experimental apparatus is studied with a GEANT-based [9] simulation of the CLEO detector, where the simulated events are processed in a fashion similar to data.

In CLEO II, the momenta of charged particles are measured with a tracking system consisting of a six-layer straw tube chamber, a ten-layer precision drift chamber, and a 51-layer main drift chamber, all operating inside a 1.5 T superconducting solenoid. The main drift chamber also provides a measurement of specific ionization energy loss, which is used for particle identification. For CLEO II.V, the six-layer straw tube chamber was replaced by a three-layer double-sided silicon vertex detector, and the gas in the main drift chamber was

changed from an argon-ethane to a helium-propane mixture. Photons are detected with a 7800-crystal CsI electromagnetic calorimeter, which is also inside the solenoid. Proportional chambers placed at various depths within the steel return yoke of the magnet identify muons.

Charged tracks are required to be well-measured and to satisfy track quality requirements based on the average hit residual and the impact parameters in both the r - ϕ and r - z planes. Muon candidates must penetrate the steel absorber to a depth of at least five nuclear interaction lengths, which effectively places a lower bound on the muon momentum of 1.2 GeV/ c . Electrons are identified by a likelihood that includes the fraction of the particle's energy deposited in the calorimeter and the spatial distribution of the deposited energy. To reduce contamination from low-momentum hadrons, the electron momentum is required to be greater than 1.0 GeV/ c . For electrons that are combined with another lepton satisfying the above criteria, the momentum requirement is lowered to 600 MeV/ c . Electron pairs from photon conversions are rejected by requiring the dielectron invariant mass to be greater than 200 MeV/ c^2 . We rely on the detector simulation to estimate the remaining contribution of hadrons to the lepton sample. π^0 candidates are formed from pairs of photons with an invariant mass within 2.5 standard deviations of the known π^0 mass that are kinematically fitted with the mass constrained to the known π^0 mass.

D mesons are reconstructed in the modes $D^0 \rightarrow K^-\pi^+$ and $D^+ \rightarrow K^-\pi^+\pi^+$, where a sum over charge conjugate modes is implied. The daughters of the D candidates must undergo ionization energy loss consistent with the particle hypothesis at the level of three standard deviations. To maximize detection efficiency, no requirements are placed on the momentum of the D candidate. We reconstruct D^* mesons in the modes $D^{*0} \rightarrow D^0\pi^0$, $D^{*+} \rightarrow D^0\pi^+$, and $D^{*+} \rightarrow D^+\pi^0$. When used in the D^* modes, D candidates must have invariant masses less than 15 MeV/ c^2 (about 2.5 standard deviations) from the known mass.

Figure 1 shows the $K^-\pi^+$ and $K^-\pi^+\pi^+$ invariant mass distributions of D^0 and D^+ candidates, respectively, associated with two oppositely charged leptons. Also shown are the normalizing distributions for D candidates paired with a single lepton of either charge. The analogous distributions for the D^* modes, showing the D^* - D mass difference, are given in Figure 2. The $D^{(*)}$ -dilepton distributions reveal a striking absence of signal. The $D^{(*)}$ yields are extracted from a fit of each histogram to a Gaussian distribution over a linear background for the D modes and a quadratic background for the D^* modes. The means and widths of the Gaussians for the $D^{(*)}$ -dilepton fit are fixed to values determined from the normalizing distributions, where the Gaussian widths are typically 6.5–7.0 MeV/ c^2 for $M(D)$ and 0.5–1.0 MeV/ c^2 for $M(D^*) - M(D)$. Table I lists the yields observed in data as well as the expected yields determined from a simulation of $e^+e^- \rightarrow q\bar{q}$ events, where $q \in \{u, d, s, c\}$, hereafter referred to as “continuum” events. No significant excess is observed in any mode.

In the normalizing distributions there is good agreement between the data and simulated continuum events. In addition, by analyzing data taken on the $\Upsilon(4S)$ resonance, we observe the closely related semileptonic B decay with yields that agree well with predictions from the detector simulation.

We determine the efficiency for detecting a supersymmetric \tilde{B} meson using Monte Carlo simulation. A range of values for the \tilde{B} mass, $M(\tilde{B})$, from 3.5 to 4.5 GeV/ c^2 , has been explored. Also, the sneutrino mass, $M(\tilde{\nu})$, was varied within the kinematically allowed range. In the process $e^+e^- \rightarrow \tilde{b}\tilde{b}^*$, followed by hadronization, the supersymmetric \tilde{B} mesons have

energies $E(\tilde{B})$ distributed from $M(\tilde{B})$ to E_{beam} according to some unknown fragmentation function, which we approximate by a delta function $\delta(E(\tilde{B}) - E_0)$, with E_0 given a value between $M(\tilde{B})$ and E_{beam} . We simulate both \tilde{B} mesons and their daughters, as well as the additional hadrons that result from fragmentation. We determine the dependence of efficiency on $M(\tilde{B})$, $M(\tilde{\nu})$, and E_0 . To simulate the decay $\tilde{B} \rightarrow D\ell^-X$, we have taken X to be a single pion and used three-body phase space for the decay. For $\tilde{b} \rightarrow c\ell^-\tilde{\nu}$, we have used $D\ell^-\tilde{\nu}$ three-body phase space.

These variations affect the \tilde{B} meson detection efficiency primarily through the lepton momentum spectrum. Table I lists a representative set of detection efficiencies and the resultant 95% confidence level upper limits on the cross section, assuming $M(\tilde{B}) = 4.0 \text{ GeV}/c^2$, $M(\tilde{\nu}) = 0 \text{ GeV}/c^2$, and $E_0 = E_{\text{beam}}$. The efficiency exhibits weak dependence on $M(\tilde{B})$, but lower values of E_0 tend to soften the lepton momentum spectrum, resulting in reduced efficiency. For the smallest value of E_0 we considered (3.7 GeV), the efficiencies are one-fourth of those with $E_0 = E_{\text{beam}}$. We give the upper limit on the product of the $\tilde{B}\tilde{B}$ production cross section and the $\tilde{B} \rightarrow D^{(*)}\ell\{\pi, \tilde{\nu}\}$ branching fraction as a function of $M(\tilde{B})$ and E_0 , assuming $M(\tilde{\nu}) = 0 \text{ GeV}/c^2$. For all modes, the variation of the efficiency with $M(\tilde{\nu})$ is roughly linear between $M(\tilde{\nu}) = 0 \text{ GeV}/c^2$ and $M(\tilde{\nu})_{\text{max}} \equiv 0.6M(\tilde{B}) - 0.8 \text{ GeV}/c^2$, where the efficiency vanishes. Hence, the upper limits for a finite $M(\tilde{\nu})$ would be those for $M(\tilde{\nu}) = 0 \text{ GeV}/c^2$, scaled by a factor $\left(1 - \frac{M(\tilde{\nu})}{M(\tilde{\nu})_{\text{max}}}\right)^{-1}$.

The detection efficiency is also affected by the additional particles produced in fragmentation. From Monte Carlo studies, we have determined that for each fragmentation particle, the fractional decrease in efficiency is approximately 3% and depends on the momentum and species of the fragmentation particles. By considering Monte Carlo simulation of $e^+e^- \rightarrow c\bar{c}$, we estimate roughly two fragmentation particles per GeV of fragmentation energy. The detection efficiency has been corrected accordingly. A systematic error per fragmentation particle of $\pm 2.5\%$ for the D modes and $\pm 5\%$ for the D^* modes has been included in the upper limits to allow for the uncertainty in this correction.

In addition, the upper limits have been inflated to account for uncertainties in the detector simulation and in the D and D^* branching fractions, which amount to systematic errors of 20%. We also assign an error of 10% to the expected Standard Model yields due to uncertainties in the simulation of both fake and real leptons. The total systematic uncertainties are small compared to the statistical errors on the background-subtracted yields.

Figure 3 shows the 95% confidence level upper limit on the product of $\sigma(e^+e^- \rightarrow \tilde{B}\tilde{B})$ and $\mathcal{B}(\tilde{B} \rightarrow D^{(*)}\ell\{\pi, \tilde{\nu}\})$ as a function of $M(\tilde{B})$ and E_0 , assuming $M(\tilde{\nu}) = 0 \text{ GeV}/c^2$. The strong rise of the upper limits with decreasing E_0/E_{beam} reflects the softening of the lepton spectrum. Because of the β^3 dependence of the cross section near threshold, the cross section at $\sqrt{s} = 10.52 \text{ GeV}$ is heavily dependent on the assumed $M(\tilde{B})$. These predicted cross sections are shown as the thick curves in Figure 3. For both the D -dilepton and D^* -dilepton signatures, the upper limits in nearly all of the kinematically allowed $M(\tilde{B})$ - E_0 parameter space with $M(\tilde{\nu}) = 0 \text{ GeV}/c^2$ fall below the predicted $\tilde{b}\tilde{b}$ production cross section. Below $M(\tilde{B}) = 3.9 \text{ GeV}/c^2$, the D^* -dilepton efficiency vanishes, so we exclude a \tilde{B} that decays $\tilde{B} \rightarrow D^*\ell\{\pi, \tilde{\nu}\}$ only in the mass range 3.9–4.5 GeV/c^2 . No portion of the parameter space is excluded if $M(\tilde{\nu})$ is greater than 1.2 GeV/c^2 and 1.3 GeV/c^2 for the D -dilepton and D^* -dilepton signatures, respectively.

If the R -parity-violating decay $\tilde{b} \rightarrow c\ell^-$ were to occur, then some fraction of the time it would appear as the dressed decay $\tilde{B} \rightarrow D\ell^-$ or $\tilde{B} \rightarrow D^*\ell^-$. We have examined the $D\ell^-$ and $D^*\ell^-$ invariant mass distributions in $D^{(*)}\ell^+\ell^-$ events for evidence of a peak indicating such two-body decays. We find no evidence of a peak. Fitting the distributions to a polynomial background plus a Gaussian with width given by our experimental resolution ($10 \text{ MeV}/c^2$), and stepping the Gaussian mean over the mass range, we obtain upper limits on the product of the $\tilde{b}\tilde{b}$ production cross section and the $\tilde{B} \rightarrow D^{(*)}\ell^-$ decay branching fraction, as a function of $M(\tilde{B})$. These upper limits, which include 15% systematic errors on the yields, are shown in Figure 3. For $\tilde{B} \rightarrow D\ell^-$, the upper limit is less than 0.3 pb for all masses except near $4.36 \text{ GeV}/c^2$, where it is 1.0 pb. For $\tilde{B} \rightarrow D^*\ell^-$ the upper limit is weaker, typically 3 pb for masses around $4 \text{ GeV}/c^2$, dropping to 0.3 pb for masses near $4.5 \text{ GeV}/c^2$.

In conclusion, we have searched for associated $\tilde{B}\tilde{B}$ production in e^+e^- collisions with center-of-mass energy below the $B\tilde{B}$ production threshold. We assume a branching fraction of 100% for $\tilde{B} \rightarrow D^{(*)}\ell^-\pi$ or $\tilde{B} \rightarrow D^{(*)}\ell^-\tilde{\nu}$. Considering D -dilepton and D^* -dilepton combinations, we find no evidence of a light scalar bottom quark produced at $\sqrt{s} = 10.52 \text{ GeV}$. Upper limits on the $\tilde{B}\tilde{B}$ production cross section depend on the assumed mass and energy of the \tilde{B} meson, as well as the mass of the sneutrino. For $M(\tilde{\nu})$ less than $\mathcal{O}(1 \text{ GeV}/c^2)$, the existence of a light scalar bottom quark with mass between $3.5 \text{ GeV}/c^2$ and $4.5 \text{ GeV}/c^2$ has been excluded at the 95% confidence level. A light scalar quark decaying 100% of the time $\tilde{b} \rightarrow c\ell\tilde{\nu}$ and/or $\tilde{b} \rightarrow c\ell$ would have escaped our notice only if its decay matrix element results in a lepton spectrum much softer than three-body phase space.

ACKNOWLEDGMENTS

We thank Tung-Mow Yan and Matthias Neubert for useful discussions. We gratefully acknowledge the effort of the CESR staff in providing us with excellent luminosity and running conditions. I.P.J. Shipsey thanks the NYI program of the NSF, M. Selen thanks the PFF program of the NSF, A.H. Mahmood thanks the Texas Advanced Research Program, M. Selen and H. Yamamoto thank the OJI program of DOE, M. Selen thanks the Research Corporation, F. Blanc thanks the Swiss National Science Foundation, and H. Schwarthoff and E. von Toerne thank the Alexander von Humboldt Stiftung for support. This work was supported by the National Science Foundation, the U.S. Department of Energy, and the Natural Sciences and Engineering Research Council of Canada.

REFERENCES

- [1] S. Pacetti and Y. Srivastava, [hep-ph/0007318](#); A. Dedes and H. K. Dreiner, [hep-ph/0009001](#).
- [2] G. Taylor, Representing the ALEPH Collaboration, LEPC Presentation, 20 July 2000, <http://alephwww.cern.ch>; D. Schlatter, Representing the ALEPH Collaboration, LEPC Presentation, 5 September 2000, <http://alephwww.cern.ch>; M. Pepe-Altarelli, Representing the LEP Collaborations, IVth Rencontres du Vietnam, Hanoi, Vietnam, 19-25 July 2000.
- [3] M. Carena, S. Heinemeyer, C. E. M. Wagner, and G. Weiglein, [hep-ph/0008023](#).
- [4] CLEO Collaboration, R. Ammar *et al.*, Phys. Rev. D **57**, 1350 (1998); E. Rice *et al.*, Phys. Rev. Lett. **48**, 906 (1982); A. Osterheld *et al.*, SLAC-PUB-4160; Z. Jakubowski *et al.*, Z. Phys **C40**, 49 (1988); Phys. Lett. **116B**, 383 (1982); B. Niczyporuk *et al.*, Z. Phys. **C15**, 299 (1982); J. L. Siegrist *et al.*, Phys. Rev. D **26**, 969 (1982); P. A. Rapidis *et al.*, Phys. Rev. Lett. **39**, 526 (1977); P. A. Rapidis, thesis, SLAC-Report-220 (1979); A. E. Blinov *et al.*, Z. Phys. **C70**, 31 (1996); A. Bäcker, thesis Gesamthochschule Siegen, DESY F33-77/03 (1977); C. Gerke, thesis, Hamburg Univ. (1979); Ch. Berger *et al.*, Phys. Lett. **81B**, 410 (1979); W. Lackas, thesis, RWTH Aachen, DESY Pluto-81/11 (1981).
- [5] U. Nierste and T. Plehn, [hep-ph/0008321](#).
- [6] D.E. Groom *et al.*, Eur. Phys. J. **C15**, 215 (2000).
- [7] CLEO Collaboration, Y. Kubota *et al.*, Nucl. Instrum Methods Phys. Res. A **320**, 66 (1992).
- [8] T. S. Hill, Nucl. Instrum. Methods Phys. Res. A **418**, 32 (1998).
- [9] R. Brun *et al.*, CERN DD/EE/84-1.

TABLE I. Fitted D and D^* yields for the $D^{(*)}$ -dilepton signature. The expected yields due to Standard Model processes are obtained from an analysis of simulated continuum events and include a systematic error of 10% due to uncertainties in the modeling of both fake and real leptons. The representative signal efficiencies given include the $D^{(*)}$ branching fractions and assume $M(\tilde{B}) = 4.0$ GeV/ c^2 , $E_0 = E_{\text{beam}}$, and $M(\tilde{\nu}) = 0$ GeV/ c^2 . The corresponding 95% confidence level upper limits on the product of the $e^+e^- \rightarrow \tilde{b}\tilde{b}$ production cross section and the $\tilde{B} \rightarrow D^{(*)}\ell\{\pi, \tilde{\nu}\}$ branching fraction are calculated from the excess in the measured yield over the expected yield. These upper limits include systematic errors of 20% on the reconstruction efficiency.

Mode	Yield	Expected Yield	ϵ_{sig} (%)	$\sigma(e^+e^- \rightarrow \tilde{b}\tilde{b}) \times \mathcal{B}(\tilde{B} \rightarrow D^{(*)}\ell\{\pi, \tilde{\nu}\})$
$D^0\ell^+\ell^-$	47.6 ± 20.0	$33.7 \pm 14.7 \pm 3.4$	0.44 ± 0.02	
$D^\pm\ell^+\ell^-$	37.4 ± 25.1	$58.3 \pm 21.3 \pm 5.8$	0.86 ± 0.04	
$D\ell^+\ell^-$				< 2.7 pb at 95% C.L.
$D^{*0}\ell^+\ell^-$	4.9 ± 3.4	$4.2 \pm 2.6 \pm 0.4$	0.08 ± 0.01	
$D^{*\pm}(D^0\pi^\pm)\ell^+\ell^-$	11.3 ± 3.8	$4.0 \pm 2.0 \pm 0.4$	0.12 ± 0.01	
$D^{*\pm}(D^\pm\pi^0)\ell^+\ell^-$	0.2 ± 3.6	$3.6 \pm 2.3 \pm 0.4$	0.09 ± 0.01	
$D^*\ell^+\ell^-$				< 3.7 pb at 95% C.L.

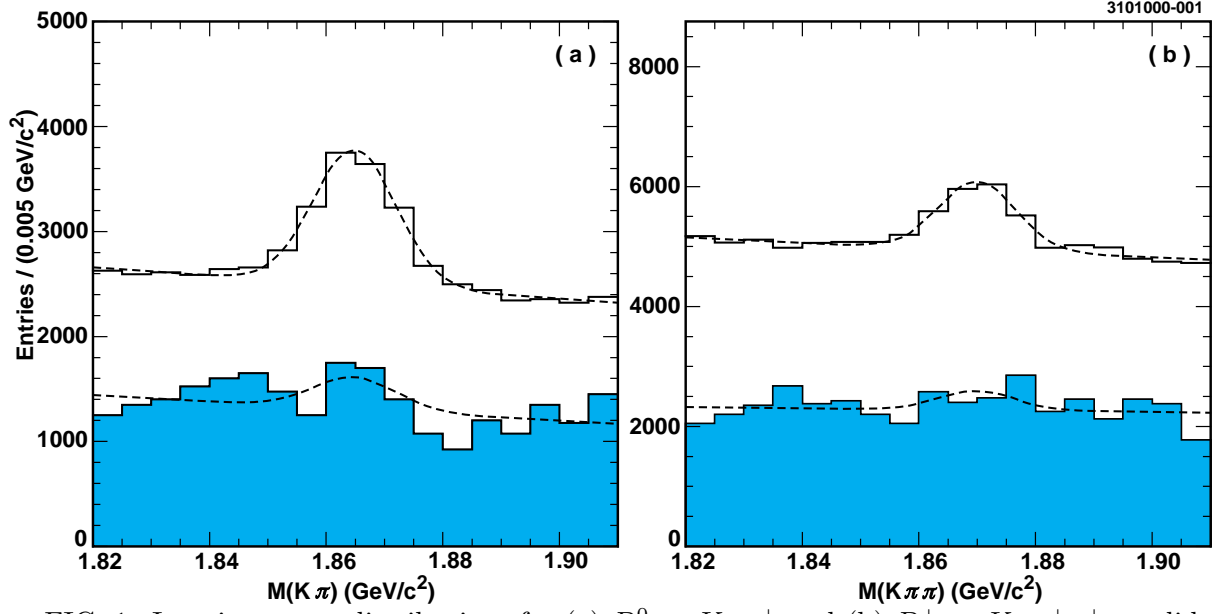


FIG. 1. Invariant mass distributions for (a) $D^0 \rightarrow K^-\pi^+$ and (b) $D^+ \rightarrow K^-\pi^+\pi^+$ candidates paired with a single lepton of either charge (open histogram) or with two oppositely charged leptons (shaded histogram). The two D -dilepton distributions have been scaled by a factor of 25 to facilitate comparison with the normalizing distributions. The fits of each distribution to a Gaussian and a linear background are shown in the dashed curves.

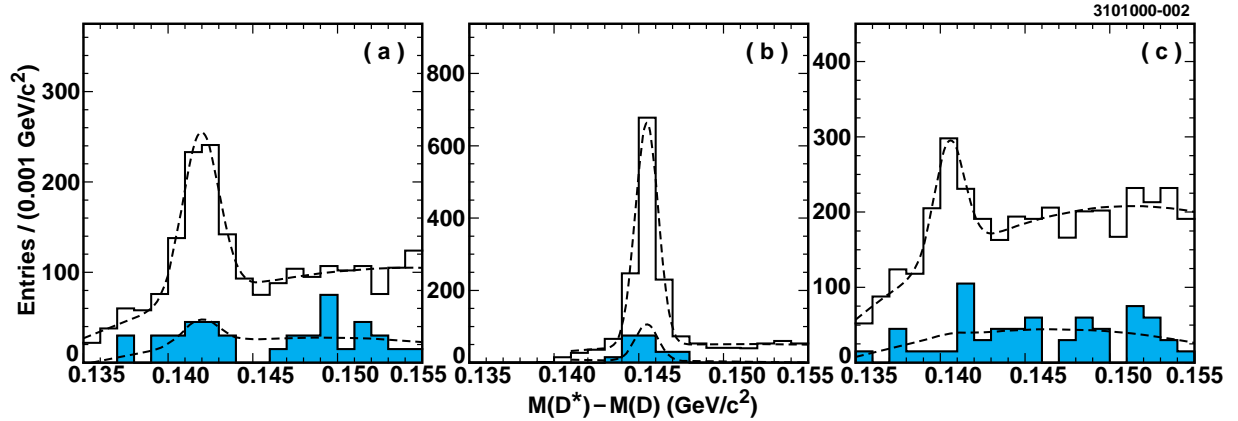


FIG. 2. Distributions of $M(D^*) - M(D)$ for (a) $D^{*0} \rightarrow D^0\pi^0$, (b) $D^{*+} \rightarrow D^0\pi^+$, and (c) $D^{*+} \rightarrow D^+\pi^0$ candidates paired with a single lepton of either charge (open histogram) or with two oppositely charged leptons (shaded histogram). The three D^* -dilepton distributions have been scaled by a factor of 15 to facilitate comparison with the normalizing distributions. The fits of each distribution to a Gaussian and a quadratic background are shown in the dashed curves.

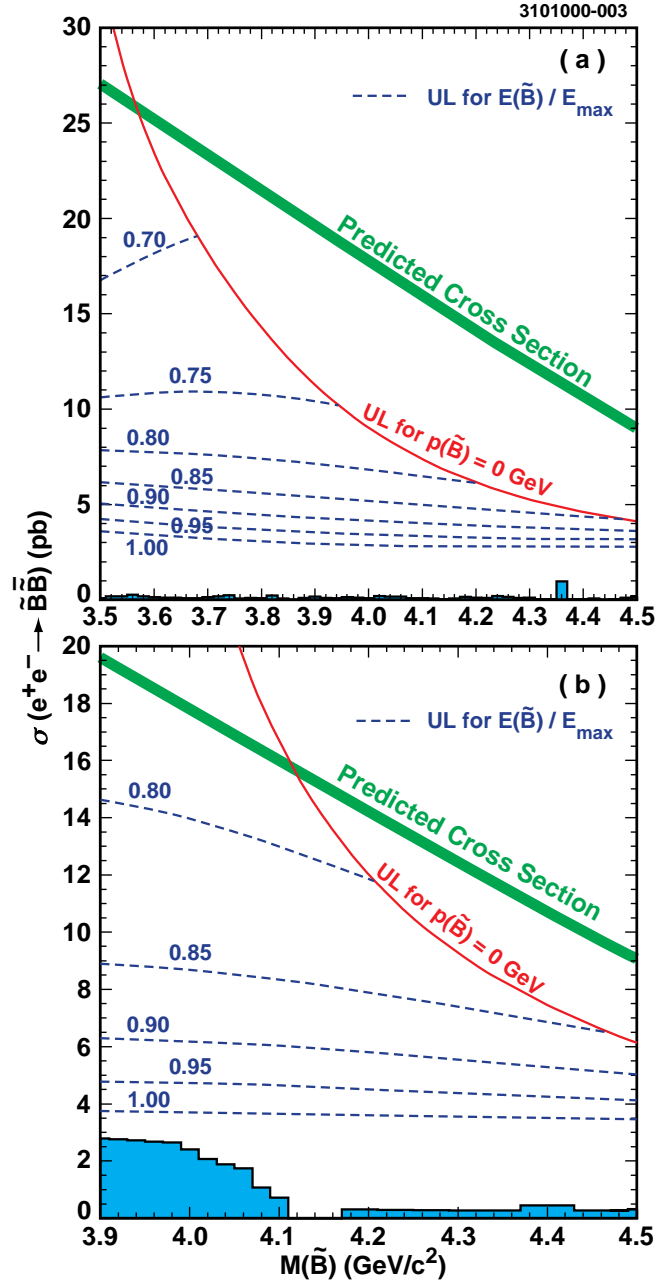


FIG. 3. Upper limits at the 95% confidence level on the product of the $e^+e^- \rightarrow \tilde{B}\tilde{B}$ production cross section and the $\tilde{B} \rightarrow D^{(*)}\ell^- \{\pi, \tilde{\nu}\}$ branching fraction. The upper limits for the (a) D -dilepton and (b) D^* -dilepton signatures are given for the full kinematic range of $E(\tilde{B})/E_{\text{beam}}$ as a function of the \tilde{B} mass, $M(\tilde{B})$, assuming $M(\tilde{\nu}) = 0$ GeV/ c^2 . The thick curves show the theoretically predicted cross sections, derived from the cross section for pointlike fermions and scaled by $\beta^3 = \left(1 - M(\tilde{B})^2/E_{\text{beam}}^2\right)^{3/2}$. For finite $M(\tilde{\nu})$, the upper limits are increased by a factor $\left(1 - \frac{M(\tilde{\nu})}{0.6M(\tilde{B}) - 0.8 \text{ GeV}/c^2}\right)^{-1}$. The shaded histograms represent the largest upper limits, for each given $M(\tilde{B})$, on an R -parity-violating \tilde{B} that decays $\tilde{B} \rightarrow D^{(*)}\ell$.